Journal of Radioanalytical and Nuclear Chemistry (2026) 335:1229–1250
https://doi.org/10.1007/s10967-025-10700-3

Gamma irradiation-induced degradation of organochlorine pesticides: groundwork for applications in cultural heritage materials

Ana Carolina Delgado Vieira[1,2] · Pablo A. S. Vasquez[2] · Maria José Alves de Oliveira[2] · Marcio Nardelli Wandermuren[3] · Joyce Cristale[4]

Received: 29 April 2025 / Accepted: 20 December 2025 / Published online: 8 January 2026

Abstract

The presence of pesticide residues in cultural heritage collections poses health risks to museum professionals, making mitigation essential. This study evaluates gamma radiation as a decontamination strategy through two complementary experiments. Standard solutions of organochlorine pesticides (dichlorodiphenyltrichloroethane, hexachlorobenzene, and lindane) were irradiated to assess degradation, while model materials (cotton, wood, vegetable fiber, and feathers) were artificially contaminated and irradiated with 30 kGy. Analyses by gas chromatography–mass spectrometry, Fourier-transform infrared spectroscopy, colorimetry, and scanning electron microscopy demonstrated pesticide degradation without significant chemical, chromatic, or structural alterations, highlighting ionizing radiation as a promising method for decontaminating cultural heritage materials.

Graphical Abstract

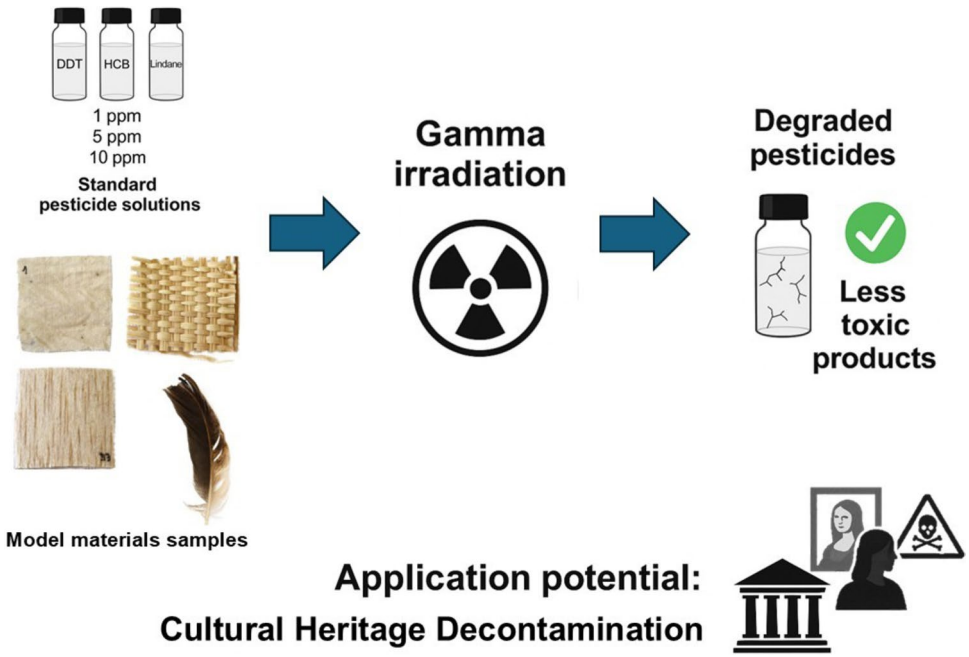

Keywords Gamma irradiation · Pesticide degradation · Decontamination · Cultural heritage

Extended author information available on the last page of the article

Introduction

Chemical treatments have long been employed for the preservation of museum collections worldwide. Since the eighteenth century, collectors and museum professionals have resorted to toxic substances, such as arsenic, mercury salts, and other biocides, to protect objects from pest-related damage. Infestations can cause scientific, cultural, aesthetic, and financial losses, which historically motivated the use of diverse chemicals. The application of herbicides, fungicides, and insecticides intensified by the late nineteenth century [1]. Synthetic organic pesticides, particularly organochlorines such as dichlorodiphenyltrichloroethane (DDT), hexachlorobenzene (HCB), and lindane (γ-HCH), were introduced and widely adopted in the mid-twentieth century, becoming common agents in the treatment of cultural heritage collections [1, 2].

Ionizing radiation has been widely studied for the degradation of organic pollutants and pesticides in environmental matrices such as wastewater, soils, and food, with numerous successful results reported [3–10].

These studies demonstrated that ionizing radiation can induce molecular bond cleavage, dechlorination, and oxidation reactions, leading to the degradation of persistent organic pollutants. Although the chemical and physical complexity of cultural heritage materials differs from that of the matrices studied in previous research, the underlying degradation mechanisms are comparable. Therefore, the results obtained in these studies provide valuable reference data for adapting irradiation parameters and understanding degradation mechanisms that could be useful for cultural heritage applications.

Despite the proven efficiency of ionizing radiation for pesticide degradation in various matrices, large-scale applications remain limited. To date, only one study [11], has experimentally investigated its use for the decontamination of model materials related to cultural heritage. That work demonstrated the feasibility of applying ionizing radiation to mock-ups contaminated with permethrin, a synthetic pyrethroid widely used in museum environments. Organochlorine pesticides, widely applied to heritage collections historically, remain unaddressed by experimental research in this specific decontamination context.

This study expands this line of research to include organochlorine compounds: DDT, HCB, and γ-HCH, aiming to provide insight into their degradation under gamma irradiation. Experimental evidence from previous investigations mentioned above suggests that relatively low absorbed doses can induce efficient degradation, supporting the feasibility of extending this technique to cultural heritage decontamination. In cultural heritage practice, absorbed doses recommended for pest and mold eradication typically range from approximately 0.5–10 kGy, with higher doses (up to ~ 25 kGy) being applied only in specific and carefully justified cases, depending on the material sensitivity and conservation objectives [12], which overlaps with the effective degradation range reported for these compounds in the scientific studies mentioned previously.

This study was carried out in two complementary experimental phases to establish both the treatment doses and the practical applicability of gamma radiation for pesticide mitigation in cultural heritage contexts. In the first phase, standard solutions of historically applied organochlorine pesticides were irradiated to isolate the fundamental effects of ionizing radiation and to generate baseline data on degradation behavior and dose optimization. This solution-based model provides an essential first step for understanding degradation mechanisms without interference from complex solid matrices. In the second phase, model materials made of cotton fabric, wood, vegetable fiber, and feathers were artificially contaminated with the same pesticides and irradiated with 30 kGy under conditions relevant to cultural heritage decontamination. Together, these experiments provide essential insights that contribute to the groundwork for future applications of irradiation in the decontamination of cultural heritage materials.

While previous studies have examined pesticide irradiation [13–15], this is the first to systematically assess organochlorine degradation in solid-state mock-ups representative of heritage materials. The experimental results obtained from these models are presented and discussed with the aim of informing future applications for the treatment of real cultural heritage objects.

Theory

Pesticides and chemical preservatives have historically been applied to museum objects through brushing, spraying, fumigation, injection, or direct powder contact [16–18]. Their use aimed both to control active infestations and to prevent future damage. Although initially conceived as a discreet and non-invasive technology [19, 20], the use of pesticides has left a problematic legacy in many museum collections.

Cultural heritage preservation manuals until the 1980s recommended the application of these pesticides to wooden objects, textiles, and other organic materials [21–25]. Currently, the conservation of cultural heritage in institutions preferably relies on non-toxic treatment techniques, combined with the implementation of integrated pest management strategies [16, 26].

Despite the lack of precise data on the half-life of pesticides, semi-quantitative assessments have been studied

[27]. The half-life is an important indicator of pesticide's persistence. Even non-persistent pesticides currently in use can remain stable in indoor environments for extended periods compared to outdoor environments, due to the absence of sunlight, humidity, or other degradation processes. In a museum environment, where pesticide-treated objects are generally stored under controlled conditions of temperature, humidity, and reduced light exposure, these conditions may be viewed as being favorable to the stability of the pesticides. In this scenario, pesticides could have a longer half-life.

Even though frequent historical application involved high concentrations, ranging from 100 ppm [18] to 25,000 ppm [28], analytical studies reveal wide variability in residue levels in museum collections, from less than 0.01 ppm to over 21,000 ppm [29]. Records documenting these treatments are often incomplete or absent, making it difficult to assess the extent of contamination [30–32]. As a result, many collections have undergone various chemical treatments with few documented records.

Physical evidence of unknown past treatments is manifested in certain objects: faded colors, powdery or crystalline residues (Fig. 1), excessive stiffness, brittle textile fibers, labels with incomplete treatment information, persistent odors, and ancient objects that appear unusually resistant to the passage of time [1, 33]. All these characteristics can indicate that pesticides were applied to ensure greater longevity for organic objects, which are often attacked by insects and fungi.

The contamination risks are not limited to professionals who handle these objects, such as conservators, curators, and researchers. Currently, the involvement of indigenous communities in museum curatorial activities has been a key element in the renewal of traditional anthropological museums. In this new context, indigenous groups visit museum storage areas and work directly with the collections housed in these institutions. In many cases, members of these communities request the use of some items for ceremonial purposes. In such situations, potential contamination of these objects restricts their use and poses a health risk to those who will physically use them. It also poses an environmental threat, as objects reintegrated into routine use may be reused in religious ceremonies or buried in the soil by indigenous community leaders [34]. Therefore, it is important to reverse or at least mitigate the contamination of these items to rehabilitate them for broader use and re-evaluate how objects were and continue to be preserved in museums.

Fig. 1 Indigenous bench with white crystalline efflorescence, treated with DDT, possibly in the 1950s. Object RG 7235 – Museum of Archaeology and Ethnology (MAE/USP). Photo: Ader Gotardo

Ionizing radiation offers a promising approach for degrading persistent organic contaminants. The mechanism involves the generation of reactive species such as hydroxyl radicals (•OH), hydrated electrons (e^-_{aq}), and hydrogen atoms (H•) through the radiolysis of water [35–37]. These reactive species can attack the chemical bonds in pesticide molecules, leading to fragmentation and the formation of less toxic byproducts. The primary degradation pathways involve dechlorination, hydroxylation, and cleavage of aromatic rings, depending on the molecular structure of the pesticide.

The absorbed dose necessary for degradation varies with the chemical nature of the contaminant and the matrix. Previous studies on environmental samples have demonstrated significant pesticide degradation at doses as low as 1–12 kGy [38–40].

This theoretical framework underpins the application of gamma irradiation as a potential method for pesticide mitigation in cultural heritage collections, aiming to achieve effective decontamination while preserving the integrity of historical materials.

Experimental

Sample preparation

The following pesticide reference materials were purchased from Dr. Ehrenstorfer (Augsburg, Germany). The family, mode of action, molecular formula, and chemical structure of the selected pesticides are as follows:

(a) Dichlorodiphenyltrichloroethane (DDT), 97.8% chemical purity: organochlorine group—insecticide/acaricide. CAS number: 50–29-3. Molecular Formula: $C_{14}H_9Cl_5$.

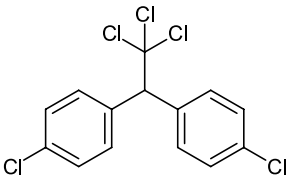

(b) Hexachlorobenzene (HCB), 99.9% chemical purity: organochlorine group—fungicide. CAS number: 118–74-1. Molecular Formula: C_6Cl_6.

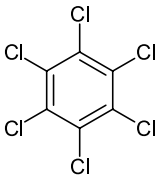

(c) Lindane (γ-HCH), 99.7% chemical purity: organochlorine group – insecticide/acaricide/rodenticide. CAS number: 58–89-9. Molecular Formula: $C_6H_6Cl_6$.

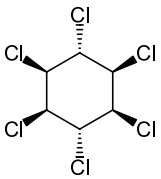

In order to prepare the diluted solutions, residue-analysis grade organic solvents (acetone and methanol) from Labsynth (São Paulo, Brazil) were used. Individual stock solutions (1,000 ppm) were prepared for each pesticide: DDT and γ-HCH were dissolved in methanol, whereas HCB was dissolved in acetone. Each compound was diluted separately using the same solvent as its reference standard. Working solutions were prepared at concentrations of 0.1, 0.2, 0.5, 1.0, 5.0, and 10.0 ppm, specifically designed for quantitative validation and calibration curve construction in GC–MS analyses. These solutions were stored in sealed, dark containers under refrigeration to minimize degradation.

The selected concentration range of working solutions used in this study was based on values reported in the literature for both applied treatments and pesticide residues found in heritage collections, as previously mentioned. Therefore, the chosen concentration range was considered realistic and representative for experimental purposes, enabling the evaluation of degradation mechanisms under controlled conditions without introducing excessive contamination that could obscure analytical interpretation.

To simulate realistic contamination scenarios in anthropological collections, representative model material samples were selected: cotton fabric (3.0 × 1.0 × 0.1 cm), buriti fiber (*Mauritia flexuosa*) (3.0 × 1.0 × 0.1 cm), balsa wood (*Ochroma pyramidale*) (3.0 × 1.0 × 0.2 cm), and chicken feathers (2.0 × 2.0 × 0.5 cm).

Each material type was individually contaminated using 10.0 ppm solutions of one of the following pesticides: DDT, HCB, and γ-HCH. Concentration was chosen as a representative value (falling within the broad range reported in museum collections) to simulate realistic contamination while ensuring controlled and comparable experimental conditions across all distinct batches of samples (Fig. 2).

Previous studies on the distribution of biocides and pesticides in porous materials guided our approach to preparing the samples (mock-ups). Unger [41] observed that up to 90% of a biocide may remain concentrated within the first 5 mm beneath the surface of a wooden artifact. In a related study, Shugar and Sirois [42] analyzed mock-ups of varying thicknesses (2.5, 5, and 10 mm) and found that the thinnest samples contained the highest arsenic concentrations, whereas thicker ones retained approximately half as much. These findings demonstrate that pesticide residues tend to accumulate near surfaces, and that thinner mock-ups may therefore overrepresent surface contamination. In light of this, the present study employed thin mock-ups to simulate surface-related contamination processes while facilitating the evaluation of decontamination efficiency.

Contamination of the mock-ups followed a standardized and reproducible procedure. Each specimen was weighed and immersed in 10 mL of a 10.0 ppm pesticide solution within an Erlenmeyer flask. The flasks were placed on a magnetic stirrer (Cienlab, Campinas, Brazil) and agitated continuously for 8 h to promote homogeneous compound penetration. After this period, samples were removed and transferred to clean beakers. Residues adhering to the flask

Fig. 2 From left to right: mock-ups made of cotton, vegetable fiber, wood, and feathers contaminated with pesticides. The figure is not to scale; actual sample dimensions are provided in the description above

walls were recovered by rinsing each vessel with 20 mL of hexane, which was added to the corresponding beaker. Samples were then air-dried at room temperature, and their final masses were recorded to detect any variation resulting from the contamination process. A separate batch of mock-ups was prepared for each pesticide to ensure that every material set was exposed exclusively to a single compound, with no mixtures.

Following contamination, the materials were divided into three experimental conditions: (a) non-irradiated controls, (b) irradiation under dry conditions, and (c) irradiation after surface humidification with distilled water. For the latter, a fine mist of distilled water was applied to the surface immediately before irradiation, while dry samples were processed without any pre-treatment.

Each specimen was placed in a zip-lock polyethylene bag that was partially closed, sufficient to prevent material loss, to ensure consistent handling and avoid cross-contamination while still allowing limited air exchange (Fig. 3).

Although the pesticides under study are poorly soluble in water [43], samples were lightly moistened before irradiation to assess the possible influence of humidity on degradation efficiency. Although humidification is generally avoided in cultural heritage treatments because of the risks it poses to sensitive materials, it may be applied by conservators under carefully controlled protocols.

Radiation processing

All irradiation experiments were conducted at the Multipurpose Gamma Irradiation Facility, a ^{60}Co gamma irradiator (IAEA Category IV) at the Radiation Technology Center (CETER/IPEN–CNEN, São Paulo). Samples were irradiated in batch mode with samples positioned in a stationary position.

In this experiment, standard pesticide solution samples at concentrations of 1.0; 5.0 and 10.0 ppm were irradiated with doses of 1, 3, 6, 10, 25, 50, and 100 kGy at a dose rate of 5 kGy.h^{-1}.

In the first stage, the solutions were placed in sealed glass vials and labeled according to their concentrations. These vials were then grouped into plastic containers based on their assigned doses, streamlining the batch processing of the material. Samples were irradiated at low temperature to maintain solution stability using artificial ice packs. No temperature monitoring was conducted, as the ice packs were used only to prevent heating and preserve the solutions under cool conditions recommended by the manufacturer.

The selected dose range (1–100 kGy) was designed to explore the relationship between absorbed dose and pesticide degradation. The lower range ($\leq$ 25 kGy) corresponds to values typically used in cultural-heritage applications such as pest and mold control, whereas higher doses (50–100 kGy) were included exclusively to assess the effect of absorbed dose on radiation-induced degradation. These upper-dose experiments were not intended for direct application to heritage artifacts, since such exposure could compromise material integrity.

For the second experiment, the irradiation doses applied to the mock-up materials were defined according to the outcomes of the preliminary tests, seeking a balance between effective pesticide removal and preservation of the substrates. The samples were exposed to a total absorbed dose of 30 kGy, delivered at a dose rate of 5 kGy·h^{-1}.

All irradiation procedures were performed in the air atmosphere, with samples placed in non-airtight plastic containers that allowed oxygen exchange, ensuring the presence of reactive oxygen species generated by radiolysis.

Absorbed doses were verified using polymethyl methacrylate (PMMA) dosimeters (Harwell Amber 3042 and

Fig. 3 Batch of wood mock-ups contaminated with 10.0 ppm DDT, separated into the three experimental conditions: **a** control, **b** dry and **c** moistened

Red 4034) and measured with a Thermo Scientific Genesys 20 UV–Vis spectrophotometer.

Pesticides analysis

Studies involving real museum collections often rely on swab sampling to quantify pesticide residues, as this represents a minimally invasive and ethically acceptable approach consistent with institutional policies and with the participation of Indigenous and originating communities in curatorial decision-making [44]. As this work was conducted with model materials rather than original artifacts, destructive analyses were employed to allow a more detailed investigation of degradation processes.

To the extraction of the contaminated mock-ups, each sample was first weighed to establish its initial mass. The specimens were then immersed in 10 mL of hexane and kept under agitation on a magnetic stirrer (Cienlab, Campinas, Brazil) for 24 h to promote complete extraction of the pesticide. Following this step, the materials were transferred to clean beakers and left to dry at room temperature. After drying, the samples were reweighed to register possible mass variations. Finally, the extracts were concentrated and re-dissolved in 0.5 mL of hexane for subsequent chromatographic analysis.

Pesticide concentrations were determined by gas chromatography–mass spectrometry (GC–MS) using a Shimadzu GC–MS 2020 system coupled with a GC–2010 quadrupole mass analyzer (Shimadzu Corporation, Kyoto, Japan). The analyses were performed with a DB-5 analytical capillary column (5% phenylsilicone, 95% methylsilicone; 30 m length, 0.25 mm internal diameter, 0.25 µm film thickness; Agilent Technologies, Santa Clara, USA; J&W Serial No. USN108762H).

The GC oven program was set as follows: the initial temperature was set to 60 °C and held for 1 min; the temperature was then increased at a rate of 10 °C/min up to 250 °C and held for 15 min. Injection was performed in split ratio mode (5.0) with an injection volume of 3 µL. Helium (99.999% chemical purity) was used as the carrier gas with a column flow rate of 1.63 ml/min. The detection parameters of the mass spectrometer are detailed in Supplementary Table S1.

Analytical method validation included assessments of selectivity, linearity, limit of detection (LOD), limit of quantification (LOQ), precision, and accuracy, following procedures described in the literature [45–48]. Linearity was evaluated by least-squares regression of calibration curves, with $R^2 \geq 0.99$ (Supplementary Figures S1-S7) as the acceptance criterion. LOD and LOQ were estimated from the standard deviation of the response (σ) and the slope of the calibration curve (s), using 3.3σ/s and 10σ/s, respectively. Precision and accuracy were assessed through replicate analyses and recovery tests, expressed as relative standard deviation (RSD %) and recovery percentage (%R), respectively. Detailed validation parameters are presented in Supplementary Tables S2–S5. Since there is no specific published standard for laboratories involved in pesticide residue control in cultural heritage objects, various documents were consulted to develop a methodology appropriate for the objectives of this study.

The radiation chemical yield (*G*-value) was calculated for each absorbed dose. *G* represents the number of radicals, excited states, or other products formed or lost in a system absorbing 100 eV of energy [49]. These results provide valuable insights into the nature of radiolytic reactions. The definition of the *G*-value is determined using Eq. (1), as defined by Kurucz et al. [50]:

$$G = \frac{[R]N_A}{D\left(6.24 \times 10^{16}\right)} \quad (1)$$

where, [R] is the difference in pesticide concentration in moles per dose of 10^{16}, D is the absorbed dose in Gy, 6.24×10^{16} is the conversion factor from Gy to 100 eV L^{-1}, and N_A is Avogadro's number (6.02×10^{23}). To calculate the *G*-value in the International System of Units (SI) (in µmol J^{-1}), the value was multiplied by 0.1036 [6, 39]. The calculation of the *G*-value considers the difference in concentration relative to the initial concentration of the solutions (0 kGy).

Samples were analyzed in triplicate for method validation, quintuplicate for standard solutions and triplicate for the model materials analysis. Mean values were used for reporting pesticide concentrations before and after irradiation. Quantification was based on calibration curves developed during method validation, and results were processed using the GCMS Postrun Analysis software (Shimadzu Corporation).

Characterization of irradiated model material samples

Colorimetric analyses were performed with a Spectrophotometer PCE-CSM 8 (PCE Deutschland GmbH, Meschede) using the CIEDE2000 system and SQC8 software (0°/45° geometry; 8 mm aperture). Before each session, white and black spectra were recorded with calibrated standards. Due to the small sample size, one central point was measured on each specimen; in feathers, the flattest region near the rachis or tip was chosen. The parameters ΔE*, ΔL*, Δa*, and Δb* were calculated to quantify color variation. ΔE* represents the overall difference in color perception, while ΔL* expresses lightness variation. Results were interpreted according to Hardeberg [51], $\Delta E^* < 3$ indicates imperceptible changes, 3–6 denotes noticeable but acceptable variation, and > 6 corresponds to unacceptable alteration.

FTIR analyses were performed with an Agilent Cary 630 ATR spectrometer, operating in the 4000–400 cm^{-1} range, with 128 scans collected at a resolution of 2 cm^{-1}. Each spectrum was recorded with air as the background, followed by baseline correction. For each sample, three independent spectra were acquired, and the average peak area values obtained from these measurements were used for analysis.

The most relevant vibrational modes were selected to monitor potential secondary effects in the analyzed materials based on FTIR–ATR measurements. In addition to the qualitative assessment obtained through visual inspection of the FTIR–ATR spectra, a complementary quantitative approach was implemented by generating plots that compare variations in the intensity of selected vibrational bands. The monitored bands were selected according to their established assignment in FTIR–ATR spectra of lignocellulosic and proteinaceous materials and their frequent use in the literature for tracking structural changes and degradation processes. For each band, mean absorbance values were calculated from the FTIR–ATR spectra and compared across experimental conditions. For irradiated samples, the results are expressed as the difference (Δ) between the mean band intensity of irradiated specimens and that of the non-irradiated control (0 kGy). For non-irradiated materials, band intensities were compared with those obtained from non-contaminated reference samples. For data treatment purposes, variations exceeding 0.05 absorbance units were considered relevant. Although no standardized thresholds for acceptable band intensity variation in FTIR–ATR analyses of cultural heritage materials are currently established in the literature, this value was adopted as an indicative criterion to support the evaluation of the results.

Eventual structural modifications in the samples were examined by Scanning Electron Microscopy (SEM). Both non-irradiated controls (0 kGy) and irradiated specimens (30 kGy), under dry and moistened conditions, were analyzed. Imaging was carried out with a Hitachi TM3000 microscope set to an accelerating voltage of 15 kV. Sample fragments were affixed to holders using conductive carbon tape, with additional strips applied to the edges to enhance conductivity and reduce charging artifacts. Micrographs were obtained at magnifications ranging between 50× and 300x.

The identification of degradation byproducts in the solid matrices was beyond the scope of the present work, due to the strong influence of matrix-derived interferences on GC–MS spectra; this aspect is addressed in detail for standard solutions and should be explored in future studies using complementary analytical approaches.

Results and discussion

Effect of ionizing radiation on removal of pesticide residues

Standard solutions

In this first experiment, the results show that, overall, higher absorbed doses are associated with greater percentage reductions in concentration. However, the degradation efficiency varied according to the chemical nature of each pesticide and its initial concentration.

DDT exhibited significant sensitivity to gamma radiation. More than 90% degradation was achieved at a dose of 1 kGy for 1.0 and 5.0 ppm solutions, and at 6 kGy for the 10.0 ppm solution. The chemical yield of radiation for DDT degradation is noted to be high across all solution concentrations (Table 1).

The 1.0 ppm solution fell below the method's detection limit (LOD = 0.05 ppm) at 100 kGy. The slightly higher degradation efficiency observed at lower pesticide concentrations can be attributed to reduced competition among DDT molecules for reactive species generated by radiolysis, such

Table 1 Residual concentrations and removal percentages of DDT at each absorbed dose. Values represent mean ± standard deviation (n = 3). Removal percentages were calculated from these mean concentrations

DDT Standard Solutions						
Absorbed dose (kGy)	1.0 ppm		5.0 ppm		10.0 ppm	
	Concentration (ppm)	Removal (%)	Concentration (ppm)	Removal (%)	Concentration (ppm)	Removal (%)
1	0.08 ± 0.01	92	0.11 ± 0.01	98	1.8 ± 1.0	82
3	0.07 ± 0.01	93	0.10 ± 0.01	98	1.0 ± 0.3	90
6	0.07 ± 0.01	93	0.10 ± 0.01	98	0.81 ± 0.10	92
10	0.07 ± 0.01	93	0.09 ± 0.01	98	0.73 ± 0.30	93
25	0.06 ± 0.01	93	0.08 ± 0.02	98	0.53 ± 0.20	95
50	0.05 ± 0.01	95	0.08 ± 0.01	98	0.48 ± 0.10	95
100	< LOD	< LOD	0.07 ± 0.01	98	0.47 ± 0.10	95

< LOD: Below the limit of detection

as hydroxyl radicals (•OH), hydrated electrons (e^-_{aq}), and hydrogen atoms (H•). Under more dilute conditions, these reactive species are more likely to interact with individual pesticide molecules rather than recombine or react with intermediates, resulting in a higher apparent degradation rate.

Chromatographic and mass spectral data indicate that DDT underwent partial degradation, yielding products consistent with dichlorodiphenyldichloroethane (DDD) and dichlorodiphenyldichloroethylene (DDE), in agreement with classical dechlorination routes reported in the literature [52] (Supplementary Figure S10).

These compounds are structural analogues of DDT that differ by the loss of chlorine and hydrogen atoms: DDD results from reductive dechlorination, while DDE is formed by dehydrochlorination. Both transformations reduce the degree of chlorination, leading to less acutely toxic metabolites. DDT and its derivatives consist primarily of C–C, C–H, and C–Cl bonds [53], and the radiolytic cleavage of C–Cl bonds promotes the formation of these less chlorinated congeners, thus potentially lowering overall toxicity.

HCB also displayed dose-dependent degradation. A reduction greater than 45% was achieved at absorbed doses between 6 and 10 kGy, depending on the initial concentration, whereas reductions exceeding 90% were obtained at 100 kGy for the 1.0 and 10.0 ppm solutions (Table 2). Although HCB degradation generally increased with absorbed dose, the 5.0 ppm solution exhibited lower degradation efficiency than the 10.0 ppm sample at 100 kGy. This apparent inconsistency may reflect solvent–solute effects in acetone (e.g., partial volatilization) and cannot exclude minor preparation variability for this batch (e.g., pipetting or adsorptive losses). Such factors could transiently limit the homogeneous availability of HCB to react with radiolytically generated radicals, producing concentration-dependent deviations.

Pentachlorobenzene (PeCB) was suggested as a potential degradation product, consistent with previous findings that radiolysis of highly chlorinated aromatic compounds may proceed via stepwise dechlorination [54, 55] (Supplementary Figure S11).

ɣ-HCH exhibited high sensitivity to gamma radiation, achieving degradation rate of more than 90% (below the LOD of 0.10 ppm) at 100 kGy for the 1.0 ppm solution. For the 5.0 ppm and 10.0 ppm solutions, degradation rates reached 88% and 84% at 100 kGy, respectively (Table 3).

Additionally, the radiation chemical yield for γ-HCH degradation is relatively more effective in less concentrated solutions. For instance, in the 1.0 ppm solution, γ-HCH concentration is reduced below the quantification limit (LOQ = 0,36 ppm) with a 10 kGy dose, whereas in the 10.0 ppm solution, the reduction is only 82% at the same radiation dose. This enhanced efficiency in dilute solutions is attributed to the more favorable stoichiometric ratio (radical-pesticide ratio) between the γ-HCH molecules and the highly reactive species generated during methanol radiolysis (e.g., $\bullet CH_2OH$), thereby reducing competition for the destructive radicals.

The isotopic pattern and fragmentation profile are consistent with chlorinated aromatics compounds, suggesting trichlorobenzenes (TCB) as degradation products of ɣ-HCH, consistent with mechanisms involving electron attachment to the chlorinated ring followed by C–Cl bond cleavage [56] (Supplementary Figure S12). As observed for DDT, solutions dissolved in methanol showed enhanced degradation efficiency, likely due to the higher yield of reactive intermediates generated by solvent radiolysis.

Pesticides can degrade through physical, chemical, and biological processes [57, 58]. For the discussion of the presented results, the focus will be on chemical phenomena. This effect depends on the chemical composition or the type of chemical bonds present in the analyte. Authors have pointed out that interaction with solvated electrons results in higher degradation yields in polar solvents compared to non-polar solvents [8, 59].

Table 2 Residual concentrations and removal percentages of HCB at each absorbed dose. Values represent mean ± standard deviation (n = 3). Removal percentages were calculated from these mean concentrations

HCB Standard Solutions						
Absorbed dose (kGy)	1.0 ppm		5.0 ppm		10.0 ppm	
	Concentration (ppm)	Removal (%)	Concentration (ppm)	Removal (%)	Concentration (ppm)	Removal (%)
1	0.89 ± 0.30	11	4.84 ± 1.0	3	10 ± 0.5	0
3	0.72 ± 0.10	28	4.35 ± 1.5	13	9.62 ± 0.30	4
6	0.53 ± 0.20	47	2.86 ± 1.8	43	9.60 ± 0.50	4
10	0.24 ± 0.10	75	2.44 ± 1.1	51	7.43 ± 0.80	26
25	0.16 ± 0.06	83	2.09 ± 0.20	58	7.24 ± 0.20	28
50	0.15 ± 0.06	85	2.06 ± 0.70	59	6.12 ± 0.70	39
100	0.07 ± 0.10	92	1.59 ± 0.40	68	0.16 ± 0.10	98

Table 3 Residual concentrations and removal percentages of γ-HCH at each absorbed dose. Values represent mean ± standard deviation (n = 3). Removal percentages were calculated from these mean concentrations

γ-HCH Standard Solutions						
Absorbed dose (kGy)	1.0 ppm		5.0 ppm		10.0 ppm	
	Concentration (ppm)	Removal (%)	Concentration (ppm)	Removal (%)	Concentration (ppm)	Removal (%)
1	0.71 ± 0.10	29	4.05 ± 0.50	19	2.87 ± 1.0	71
3	0.62 ± 0.20	38	3.67 ± 1.0	27	2.65 ± 1.2	74
6	0.57 ± 0.10	43	3.10 ± 0.70	38	2.65 ± 0.40	74
10	< LOQ	< LOQ	3.02 ± 0.40	40	2.62 ± 0.60	74
25	< LOQ	< LOQ	2.09 ± 0.40	58	2.57 ± 0.40	74
50	< LOQ	< LOQ	1.27 ± 0.40	75	1.83 ± 0.50	82
100	< LOD	< LOD	0.61 ± 0.30	88	1.62 ± 0.80	84

< LOD: Below the limit of detection

The solvents used for preparing the solutions are polar and therefore contribute to the chemical yield of radiation. However, the behavior of methanol (CH_3OH) and acetone (C_3H_6O) differs significantly. The highly reactive species generated during the radiolysis of these solvents can interact with the analytes, initiating their degradation.

When methanol is exposed to ionizing radiation, radiolysis occurs, leading to the formation of reactive species such as hydroxyl radicals (•OH), hydrogen radical (H•), and methyl (•CH_3) or hydroxymethyl (•CH_2OH) radicals [60]. Although methanol can act as a scavenger of hydroxyl radicals, its radiolytic products remain chemically active and can promote degradation through hydrogen abstraction and dechlorination reactions. In addition, secondary oxidation and reduction reactions within the solvent system may sustain degradation chains, further enhancing the breakdown of analytes.

In the case of acetone, radiolysis generates acetyl (CH_3CO•) and methyl radicals (•CH_3), which tend to undergo self-reactions or recombination, forming more complex and less degradable byproducts [61]. These acetone-derived radicals can react with pesticide fragments, leading to the formation of stable, high-molecular-weight compounds that are poorly susceptible to further radiolytic degradation. This behavior may explain the lower degradation efficiency observed for HCB solutions compared to those prepared in methanol.

Considering these differences, it can be inferred that the solvent used in pesticide preparation can be a key factor influencing degradation efficiency. In this study, DDT and γ-HCH were dissolved in methanol, whereas HCB was dissolved in acetone. For DDT, doses of 1 kGy across all concentration ranges resulted in significant degradation percentages. γ-HCH showed a similar response, demonstrating high degradation efficiency with the same 1 kGy dose. In the case of HCB, the 10.0 ppm solution required a dose of 100 kGy to be nearly completely degraded. Pesticide solutions prepared in methanol exhibited higher radiolytic degradation rates at lower absorbed doses, likely due to the generation of simpler, more reactive radicals that favor analyte breakdown, compared to the more complex degradation pathways and the formation of stable byproducts associated with acetone. These solvent effects also help explain the concentration-dependent degradation trends observed in this study, as the availability and reactivity of solvent-derived radicals directly influence pesticide breakdown efficiency at different concentrations.

The efficiency of pesticide removal can be quantitatively assessed by the radiation chemical yield (*G*-value), which expresses the number of molecules degraded per 100 eV of absorbed energy. At lower doses, *G*-values were higher, indicating more efficient degradation per unit of energy deposited in the system. As the absorbed dose increased, *G*-values declined markedly, reflecting the progressive consumption of the parent pesticide molecules and the increasing competition from radiolytically generated intermediates (Supplementary Table S6). This trend has also been reported in studies involving the radiolytic degradation of halogenated organics, where secondary reactions between intermediates and radicals become dominant at higher doses [39].

The decline and stabilization of *G*-values above approximately 25 kGy indicate that most of the original pesticide molecules have already been degraded, and that further irradiation mainly promotes reactions among intermediate species, leading to secondary products rather than additional removal of the target compound. From a practical standpoint, this behavior is particularly relevant for cultural heritage applications, where maintaining the structural and visual integrity of objects is critical. The observed dose–response behavior and *G*-value trends suggest that radiation treatments for contaminated heritage collections should prioritize achieving sufficient decontamination at the lowest feasible dose. Once the degradation curve begins to plateau (Supplementary Figures S7 to S9), as indicated by stabilized

G-values, further increases in dose yield diminishing returns in decontamination efficiency and heightened risks of physical alteration. These results established the experimental basis for the second phase of this study, guiding the selection of irradiation conditions applied to model material samples representative of heritage-relevant substrates.

Comparison of the acute oral toxicity (LD_{50}) values between the original pesticides and their potential degradation products suggests that ionizing radiation leads to the formation of less toxic substances (Table 4). Degradation products such as DDD, DDE, pentachlorobenzene (PeCB), and trichlorobenzene (TCB). exhibit significantly higher LD_{50} values compared to their parent compounds, indicating lower acute toxicity. However, acute toxicity represents only part of the toxicological profile. Chronic exposure effects and environmental persistence must also be considered. Compounds such as PeCB are classified as persistent organic pollutants (POPs) under the Stockholm Convention, due to their bioaccumulative nature and long environmental half-lives.

Therefore, while gamma irradiation may reduce acute toxicity by promoting molecular breakdown, the formation and persistence of certain chlorinated byproducts highlight the need for complementary toxicity assessments and cautious interpretation of decontamination outcomes. It should also be noted that the identification of degradation products in this study was based on the visual inspection of chromatographic profiles and comparison of characteristic mass fragmentation patterns, rather than direct analysis against certified reference standards.

Model materials samples

Considering the results obtained in the first phase experiments, the irradiation dose of 30 kGy was selected for the model materials as an optimal compromise between effective pesticide degradation and preservation of the substrate integrity. Doses above 25 kGy showed a decline in *G*-values, indicating a change in radical reactivity and an increased tendency for interaction with intermediate species rather than with the parent pesticide molecules.

The choice of 30 kGy also reflected the heterogeneous composition of the model substrates, which may respond differently to ionizing radiation than homogeneous liquid solutions. Although this dose is slightly higher than those typically employed for routine disinfection of artworks, it has been reported to cause no significant adverse effects on cultural heritage materials and is also used in the polymerization of resins for the consolidation of fragile artifacts, with reported applications reaching up to 40 kGy [12]. Although standard-solution experiments identified approximately 25 kGy as an efficient degradation threshold, a slightly higher dose was adopted to verify whether similar or enhanced effects could be achieved in solid matrices. This approach provided additional insight into the role of material heterogeneity in radiolytic processes and generated data more directly relevant to real-world applications in the decontamination of cultural heritage materials. Furthermore, excessive doses could potentially induce undesirable physical or chemical alterations in the materials, such as color shifts, microstructural damage, or secondary degradation.

The overall results (Fig. 4) demonstrated that gamma irradiation was effective in degrading the three tested pesticides, although the extent of removal varied according to the substrate and the irradiation conditions. GC–MS analyses of the model material samples were performed in triplicate for each condition (control, dry irradiation, and moistened irradiation). Representative chromatograms are presented in the Supplementary Material S13-S24. The reported degradation values correspond to the mean peak areas of the triplicate analyses.

For DDT, the treatment achieved high removal rates in vegetable fiber (69% dry, 95% moist) and in cotton fabric, where complete degradation was observed under dry conditions (100%), though efficiency was lower under moist irradiation (64%). Wood exhibited moderate removal efficiency, with degradation values increasing from 23% under dry to 69% under moist conditions, suggesting that the presence of moisture enhanced the formation of reactive species and improved contaminant accessibility within the porous matrix. In contrast, feathers showed limited removal (21–45%), highlighting their lower responsiveness to the treatment (Fig. 4).

Table 4 Comparison of the toxicity of irradiated pesticides and their potential degradation products [62, 63]

Pesticide	Stockholm Convention Status	Mammals—Acute oral LD_{50} (mg kg^{-1})	Possible degradation product	Stockholm Convention Status	Mammals—Acute oral LD_{50} (mg kg^{-1})
DDT	Annex B (restricted use)	87	DDD	Not listed	600
			DDE		880
HCB	Annex A + C (elimination & unintentional release)	10	PeCB	Annex A + C	1125
γ-HCH	Annex A (elimination)	76	TCB	Not listed	1830

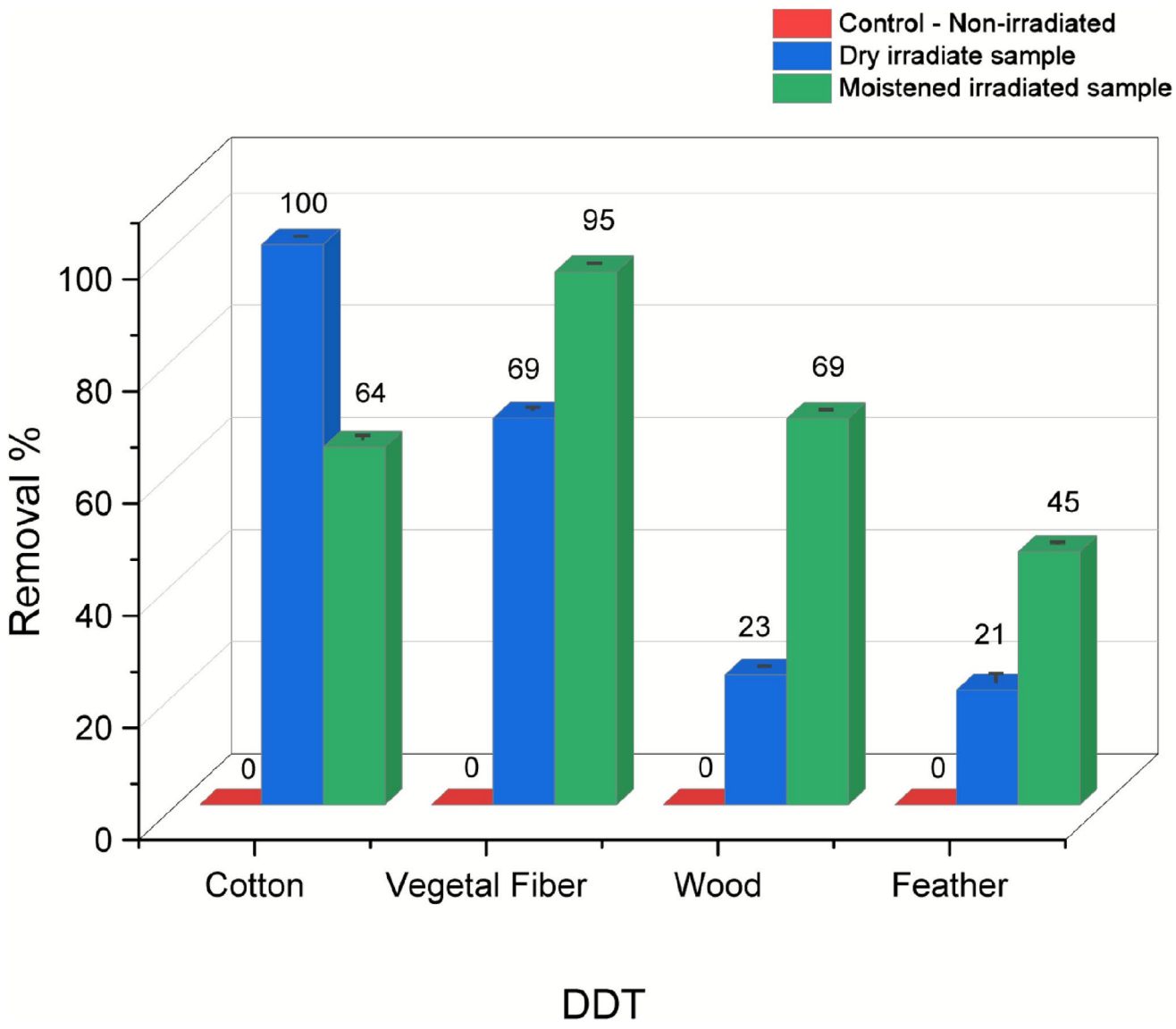

Fig. 4 Removal (%) of DDT under different processing conditions of the model material samples at 30 kGy. The values represent the average of three repetitions and their SD

For HCB, removal was consistently high across substrates, reaching complete degradation in vegetable fiber under dry conditions and in cotton fabric in both conditions (99–100%). Feathers showed little difference between dry and moist irradiation (90% and 88%), indicating high susceptibility of this pesticide to radiolytic degradation. In contrast, wood exhibited lower removal efficiency, particularly under moistened conditions (70% and 34%, respectively), suggesting that its denser structure and lower porosity may have limited the penetration of reactive species and, consequently, the overall degradation yield (Fig. 5).

For γ-HCH, however, gamma irradiation proved less efficient overall. While cotton fabric again showed nearly complete removal (99% in both conditions), the other substrates exhibited markedly lower values, confirming the higher persistence of this pesticide. In vegetable fiber, removal decreased significantly under moist conditions (48% dry, 21% moist), suggesting that the presence of water may have altered radical availability or diffusion within the matrix. Similarly, wood showed moderate efficiency (38% dry, 15% moist), while feathers displayed minimal degradation ($\leq 4\%$), consistent with their compact and low-polarity surface characteristics. These results indicate a strong resistance of γ-HCH to radiolytic breakdown across most substrates (Fig. 6).

Detailed concentration values of the irradiated samples are provided in Supplementary Table S6.

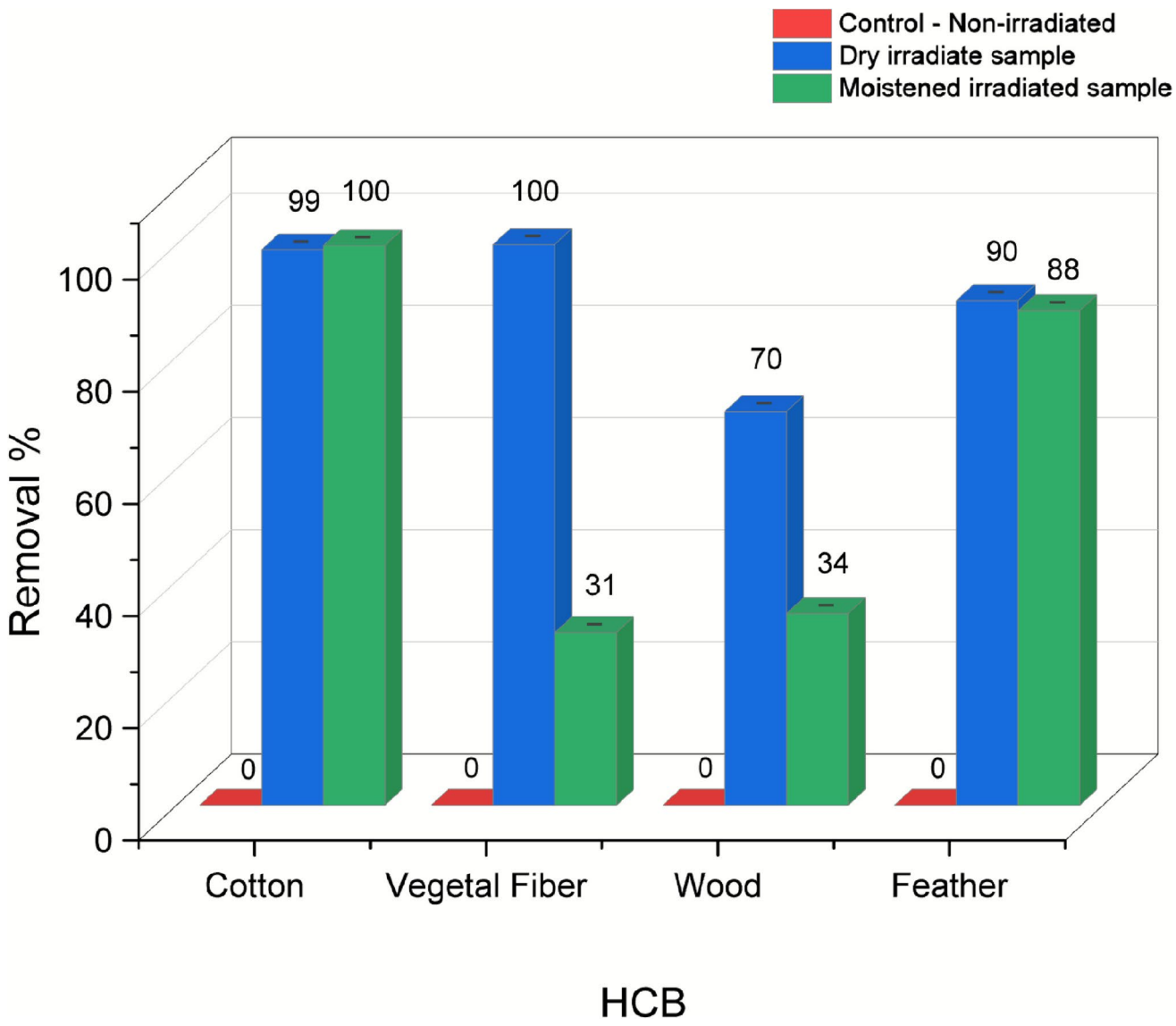

Fig. 5 Removal (%) of HCB under different processing conditions of the model material samples at 30 kGy. The values represent the average of three repetitions and their SD

Among the compounds studied, the overall average degradation rate, HCB showed the highest degradation rate (77%), followed by DDT (61%) and γ-HCH (41%). Substrate characteristics also played an important role. Cotton and vegetable fiber showed higher removal rates (93% and 61%, respectively) than wood (51%) and feathers (45%). The degradation efficiency of the organochlorine pesticides studied was strongly influenced by their molecular structure and physicochemical properties, particularly the degree of chlorination, aromaticity, and hydrophobicity. Among the compounds analyzed, HCB and DDT exhibited the highest removal rates, whereas γ-HCH showed a similar overall trend (greater efficiency under dry conditions) but with significantly lower degradation percentages.

HCB, composed of a fully chlorinated benzene ring, combines high chemical stability with strong susceptibility to direct radiolysis. Its high electron density and molecular symmetry favor efficient energy absorption and subsequent C–Cl bond cleavage even in the absence of water. The process is largely independent of solubility, which is extremely low (≈ 0.0047 mg L^{-1}) [43]. Consequently, HCB degradation reached nearly complete removal in most substrates, particularly in cotton and vegetable fiber, while slightly lower efficiencies were observed in wood samples. This difference may be associated with the denser structure and higher lignin content of wood, which could limit the diffusion of reactive species and the mobility of pesticide molecules within the matrix.

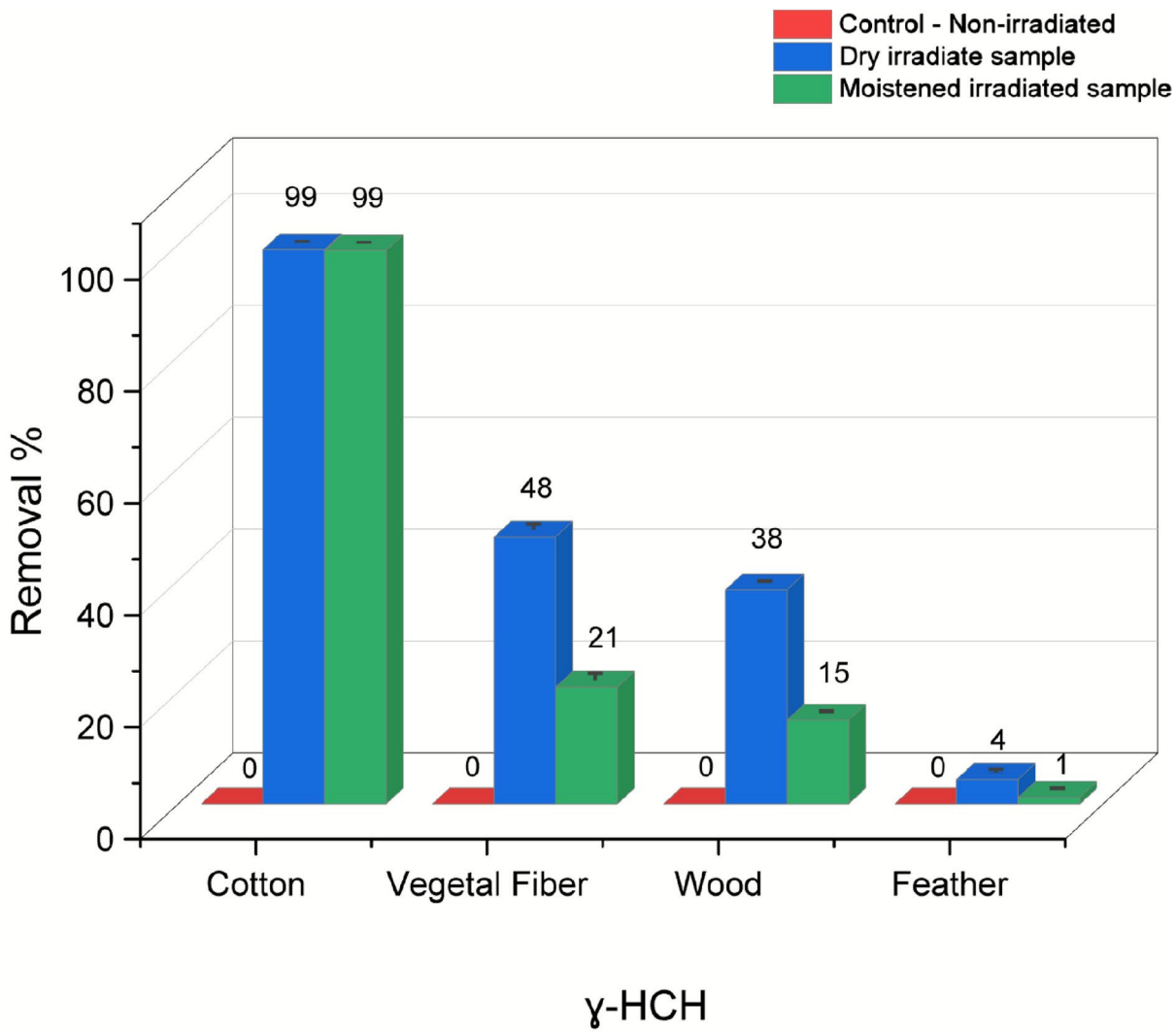

Fig. 6 Removal (%) of HCB under different processing conditions of the model material samples at 30 kGy. The values represent the average of three repetitions and their SD

DDT, although less chlorinated, also contains two aromatic rings that stabilize intermediate radicals formed during irradiation. Its degradation was enhanced under moistened conditions, in which hydroxyl radicals (•OH) derived from water radiolysis promote oxidative and stepwise dechlorination reactions. With a slightly higher water solubility (≈0.006 mg L^{-1}) [43], DDT molecules can partially interact with moisture layers within the substrates, facilitating indirect radiolysis via radical attack. The presence of thin water films on humidified substrates probably enhances radical transport and accessibility. This key factor explains the higher degradation rates observed in moist samples, particularly in wood, vegetable fiber and feathers.

In contrast, γ-HCH, despite being substantially more soluble in water (≈8.5 mg L^{-1}) [43], has a saturated, non-aromatic cyclohexane structure that limits electron delocalization and susceptibility to oxidative attack. Its saturated, non-aromatic molecular configuration hinders the stabilization of reactive intermediates, leading to slower and less efficient degradation. Its degradation occurs mainly through stepwise dechlorination, a process that is also more sensitive to matrix effects. In complex matrices such as wood and feathers, which are rich in lignin and keratin, competition for reactive radicals may further contribute to the lower degradation efficiency observed.

Thus, while HCB and DDT achieved nearly complete degradation under the applied experimental conditions, γ-HCH displayed higher resistance, with only partial removal in lignocellulosic and proteinaceous substrates and

significant degradation only in cotton fabric, whose cellulose matrix is chemically less reactive toward free radicals.

Overall, these findings reinforce that although all organochlorine pesticides are susceptible to ionizing radiation, the dominant degradation mechanism (direct *versus* indirect radiolysis) depends more on molecular structure than on solubility. Consequently, the differences observed among substrates and irradiation conditions reflect the balance between radical accessibility, molecular reactivity, and matrix composition.

Colorimetric analyses revealed that gamma irradiation generally produced only minor alterations in the visual appearance of the tested materials (Fig. 5), with almost all ΔE* values remaining below the perceptibility threshold (ΔE* < 3). Detailed values of ΔE*, Δa*, Δb*, and ΔL* for all samples are provided in Supplementary Table S7. The graphs presents average values, assuming a standard reading error of ± 0.01%.

For DDT, irradiated samples exhibited generally minor color changes, with moist irradiation tending to better preserve the original color appearance in most substrates. The main exception was feathers under moist conditions, which showed higher ΔE* values (Fig. 7a), indicating a perceptible but still acceptable color variation.

Chromatic analysis (Δa*, Δb*) revealed that irradiation predominantly induced a shift toward yellow across most substrates, suggesting a common irradiation-related effect (Fig. 7b). Deviations from this trend were observed for vegetal fiber under moist conditions, which showed a displacement toward the blue region (negative Δb*). In contrast, feathers, under both dry and moist conditions, exhibited a more pronounced shift toward the blue–green region (negative Δa* and Δb*), indicating a distinct chromatic response compared to the other substrates.

For HCB, colorimetric changes were generally limited across all substrates, with ΔE* values remaining below the perceptibility threshold under both dry and moistened conditions (Fig. 8a).

Chromatic analysis (Δa*, Δb*) revealed that irradiation of HCB-contaminated samples predominantly resulted in a shift toward the yellow region (positive Δb*) across most substrates, suggesting a consistent irradiation-related chromatic response (Fig. 8b). Minor variations in hue were observed depending on substrate and irradiation condition. Vegetal fiber and wood showed slight shifts toward the red–yellow quadrant, while feathers, especially under moist conditions, exhibited a more pronounced displacement toward higher Δb* values. Cotton under moistened conditions exhibited a slight chromatic deviation toward the green–blue region, differing from the predominantly yellow shift observed in the other substrates.

For γ-HCH, colorimetric changes were more pronounced and strongly dependent on both substrate and irradiation condition. While cotton and vegetal fiber showed moderate ΔE* values, moist irradiation of wood resulted in a clear increase in total color difference, exceeding the perceptibility threshold. Feathers also exhibited noticeable alterations, particularly under dry irradiation (Fig. 9a).

Chromatic analysis (Δa*, Δb*) indicates a more scattered response compared to DDT and HCB, with no dominant

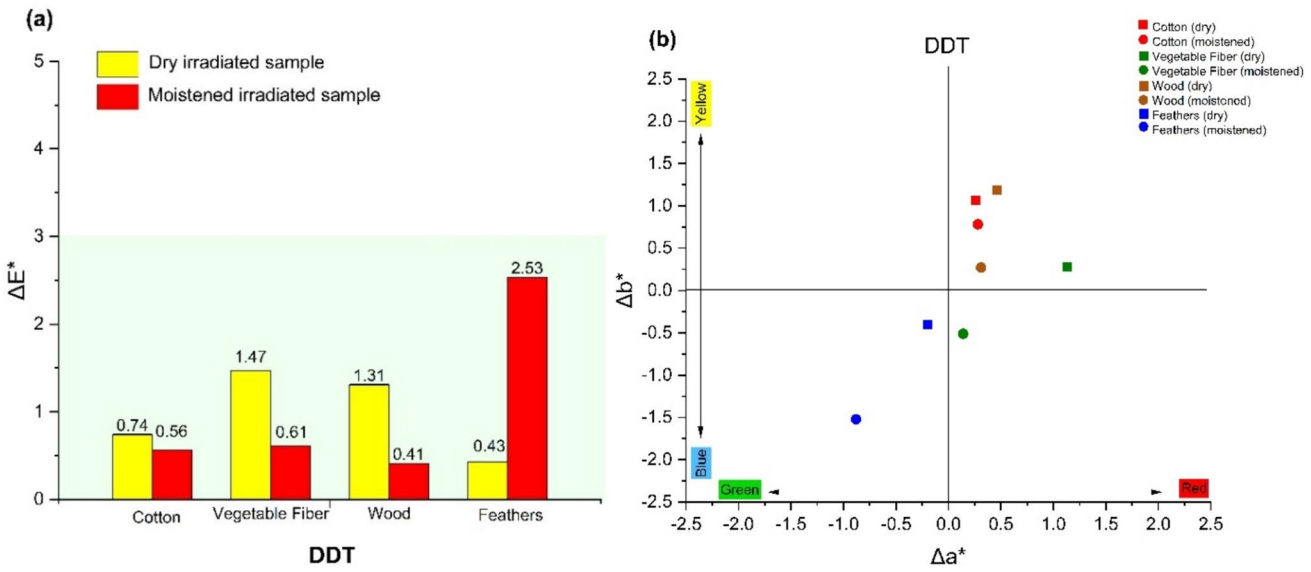

Fig. 7 Colorimetric variation of DDT-contaminated model materials after gamma irradiation. **a** Total color difference (ΔE*) for cotton, vegetal fiber, wood, and feather under dry and moistened conditions. **b** Chromatic variation (Δa* vs Δb*) of the same DDT-contaminated model materials after gamma irradiation

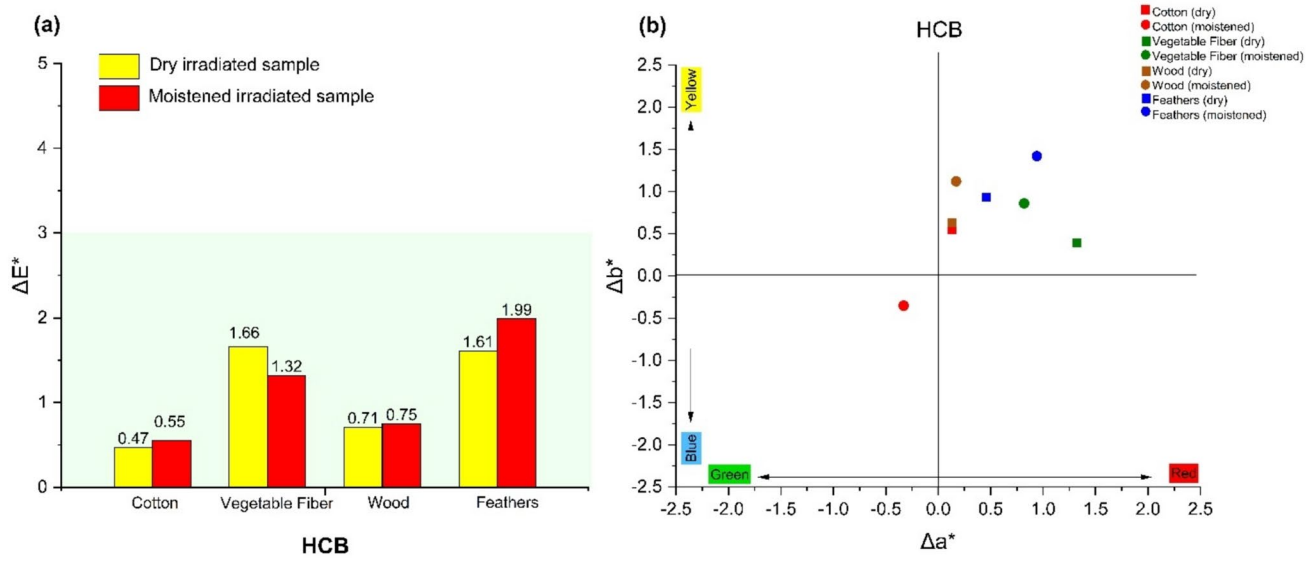

Fig. 8 Colorimetric variation of HCB-contaminated model materials after gamma irradiation. **a** Total color difference (ΔE*) for cotton, vegetal fiber, wood, and feather under dry and moistened conditions. **b** Chromatic variation (Δa* vs Δb*) of the same HCB-contaminated model materials after gamma irradiation

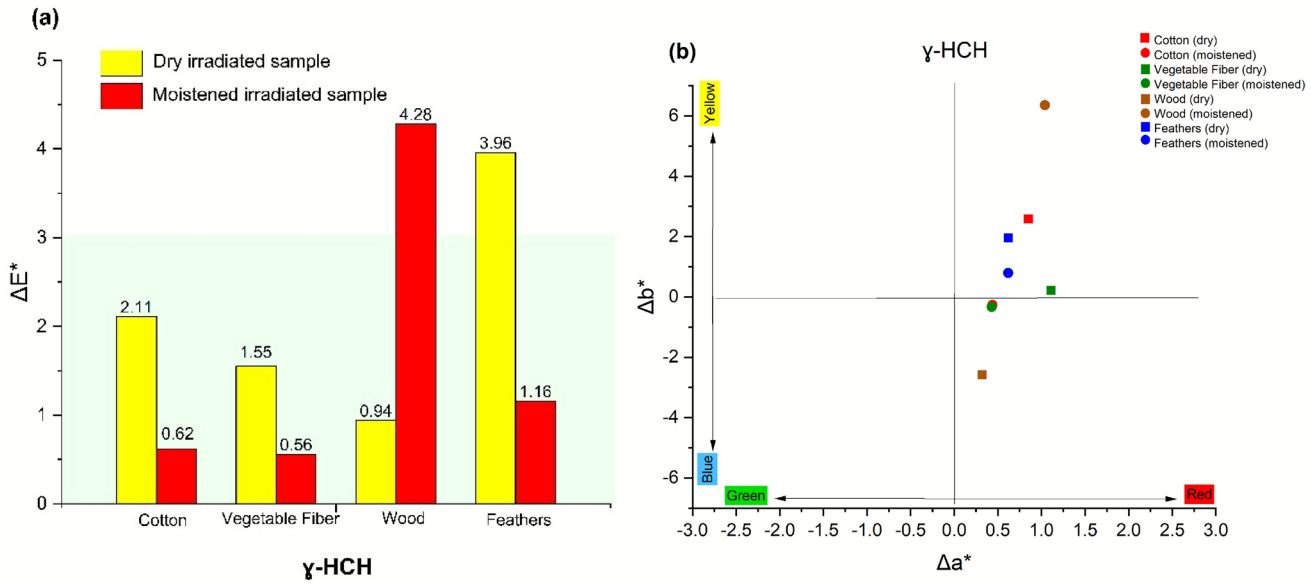

Fig. 9 Colorimetric variation of γ-HCH-contaminated model materials after gamma irradiation. **a** Total color difference (ΔE*) for cotton, vegetal fiber, wood, and feather under dry and moistened conditions. **b** Chromatic variation (Δa* vs Δb*) of the same HCB-contaminated model materials after gamma irradiation, illustrating hue shifts for cotton, vegetal fiber, wood, and feather

trend toward yellowing (Fig. 9b). Overall, these results reinforce that γ-HCH shows a higher propensity for visually perceptible changes in certain substrates highlighting its more complex interaction with both radiation and material matrices contaminated with this pesticide.

Colorimetric analyses indicated overall stability across most materials, with the exception of γ-HCH and the moistened wood and dry feather samples, which exhibited more pronounced color variations. These alterations may be linked to the generation of hydroxyl radicals (•OH) during water radiolysis. In the presence of oxygen, these radicals can form highly reactive peroxides that contribute to the degradation of organic substances [64].

Although most colorimetric measurements remained within the perceptibility threshold of $\Delta E^* < 3$, suggesting only moderate changes, visual inspection revealed

significant alterations outside the measured areas. In particular, moistened textiles and moistened vegetable fibers displayed localized signs of oxidation, especially along their edges, which were not fully captured by instrumental measurements (Fig. 10).

This underscores the importance of complementing colorimetric data with visual examination, as the latter can reveal subtle surface alterations that may be relevant for conservation decision-making process.

FTIR analyses confirmed that the degradation of organic substrates under irradiation can be tracked through variations in characteristic vibrational bands. As reported in the literature, the initial decomposition of most organic compounds involves cleavage of C–H bonds [65], an effect that can be detected by FTIR. In cellulose-based materials, monitoring C–O–C and C=O bands provides direct evidence of polymeric degradation, since changes in their intensity reflect a decrease in the degree of polymerization due to glycosidic bond rupture and oxidative processes [66–70]. In this study, vegetable fibers proved particularly sensitive, with marked changes at 2920 cm^{-1} (C–H), 1162 cm^{-1} (C–O–C), and 1029 cm^{-1} (C–O), indicating their vulnerability to irradiation under moist conditions. Similarly, variations observed in bands attributed to protein components, such as Amide I and II, suggest structural modifications in protein-rich materials [70–73], and are commonly used to monitor denaturation and degradation processes, as in the case of featherwork.

Among the evaluated materials, vegetable fibers and feathers proved to be the most susceptible to alterations induced by irradiation under moist conditions. Composed of cellulose and keratin, respectively, these materials exhibited changes in bands associated with C–H, C–O, C–O–C stretching and Amide I and II, suggesting greater vulnerability to the combined action of organic contaminants and free radicals generated during processing. An important aspect concerns the vegetable fiber samples and the bands at 2920 cm^{-1} (C–H), 1162 cm^{-1} (C–O–C), and 1029 cm^{-1} (C–O), which proved particularly sensitive to induced alterations. Monitoring their intensity allowed for distinguishing the different responses of the materials to irradiation, contributing to a more accurate assessment of the secondary effects of the treatment.

Protein-based substrates also showed susceptibility, particularly feathers, where reductions in Amide I, II, and III bands were detected. Such decreases in absorbance are commonly associated with keratin degradation, reflecting peptide chain cleavage, protein fragmentation, and reduction in molecular weight [71]. According to these authors, both the secondary and primary structures of proteins can be affected: the former through disruption of hydrogen bonds and the latter through oxidation of carbonyl and amide groups. By contrast, cotton and wood were more resistant, exhibiting only minor variations in characteristic bands under the same conditions. These findings confirm that vegetable fibers and feathers are the most susceptible substrates, particularly when irradiated under moist conditions, whereas cotton and wood maintain higher stability. The main alterations observed are summarized in Table 5 and the FTIR spectra are available in Supplementary Material S13-15.

Although infrared spectroscopy is widely employed to monitor structural changes in cellulosic and proteinaceous materials, the derivation of direct quantitative degradation parameters from FTIR data remains challenging. There are no normative standards indicating, for example, that a given percentage reduction in a vibrational band can be unequivocally interpreted as evidence of degradation. This limitation is well recognized in the literature, which recommends the use of FTIR primarily as a qualitative or semi-quantitative analytical tool [74]. Nevertheless, several studies (including the present one), consider variations in band intensity to be a valid indicator of degradation processes, particularly when evaluated in conjunction with complementary analytical evidence.

Based on the results presented in this section, and in agreement with the colorimetric data presented previously,

Fig. 10 Cotton sample contaminated with HCB, irradiated under moist conditions, shown before (left) and after (right) irradiation, exhibiting oxidation along the lower edge

Table 5 Variations in band intensities under ionizing radiation exposure. The symbol ↓ indicates a decrease in band intensity, whereas ↑ indicates an increase

Pesticide	Material	Trend under moist irradiation	Trend under dry irradiation
DDT	Vegetable Fiber	2920 (C-H) ↑	No change
	Wood	No change	1031 (C-O) ↑
	Feathers	No change	No change
	Cotton	No change	No change
HCB	Vegetable Fiber	2920 (C-H) ↓, 1732 (C = O) ↓, 1242 (C–O–C) ↓, 1162 (C–O–C) ↓ e 1029 (C-O) ↓	No change
	Wood	No change	No change
	Feathers	No change	1522 (N–H/C–N) Amida II ↑ e 1626 (C = O) Amida I ↑
	Cotton	3330 (O–H) ↓, 1160 (C–O–C) ↓ e 1030 (C-O) ↓	No change
γ-HCH	Vegetable Fiber	2920 (C-H) ↑, 1732 (C = O) ↑, 1162 (C–O–C) ↑ e 1029 (C-O) ↑	2920 (C-H) ↑
	Wood	No change	1031 (C-O) ↓
	Feathers	1626 (C = O) Amida I ↓	No change
	Cotton	No change	No change

a clear distinction was observed between samples processed under dry and moist irradiation conditions. Moist irradiation was consistently associated with a stronger tendency toward visual and structural alterations. This can be explained by the radiolysis of water, which generates reactive species such as hydroxyl radicals (•OH), hydrogen atoms (•H), and aqueous electrons (e^-_{aq}). These species readily promote oxidation reactions and induce the cleavage of structural bonds within the substrates [36]. As further noted by Sistach and Ferrer [75], oxidation processes alter hydrogen bonding and modify the availability of chemical groups, particularly through the reduction of hydroxyl functionalities, reinforcing the interpretation that oxidative processes were more likely to occur in moist-irradiated samples.

In contrast, dry-irradiated samples did not exhibit the appearance of new relevant bands, suggesting that this condition did not lead to the formation of new functional groups, significant spectral shifts, or extensive degradation of the matrices. The only exception was a band detected at ~ 2364 cm^{-1}, observed exclusively in cotton samples contaminated with HCB and irradiated. Although its precise origin could not be fully determined, this feature may be related to CO_2 adsorption or to a vibrational contribution from the contaminant itself, without clear evidence of structural damage to the material.

Overall, fabric and wood samples demonstrated higher resistance to degradation under the tested conditions, with only minor variations in the intensities of characteristic bands, even under moist irradiation. Their stability may be attributed to the lower availability of reactive groups or to the compact structure of lignocellulosic matrices. By contrast, vegetable fibers and feathers were more prone to structural changes when irradiated in the presence of moisture. These findings indicate that moist irradiation can trigger variable effects depending on the nature of the substrate, the contaminant present, and the interaction of radiolysis products with the matrix. In the context of cultural heritage conservation, the practice of pre-humidifying materials to enhance contaminant degradation should therefore be approached with caution, as it may result in undesirable secondary effects. Dry irradiation, on the other hand, proved to be the most stable and reliable condition, preserving the spectroscopic and chemical integrity of the majority of the analyzed substrates.

SEM analyses were performed at different magnification levels and across distinct regions of the artificially contaminated model material samples, including the surface and, in the case of wood, fractured cross-sections. These varied points of analysis were recorded in order to investigate whether ionizing radiation processing could induce structural or topographical changes in the samples, both in non-irradiated controls and in those irradiated under dry and moist conditions.

In the cotton sample, the intact ligaments that form the weft and warp of the fabric structure are clearly visible, as well as in the vegetable fiber sample. The wood mock-up displays, in the fractured cross-section, the vessels and fibers that comprise their anatomical structure. Similarly, in the feathers sample, the rachis, barbules, and pennaceous barbs remain well-preserved. Figure 11 illustrates the monitored areas in this experiment.

A comparison revealed that these structures were perfectly preserved following irradiation. The topographic features of the irradiated samples showed no signs of damage, even when exposed to different irradiation conditions.

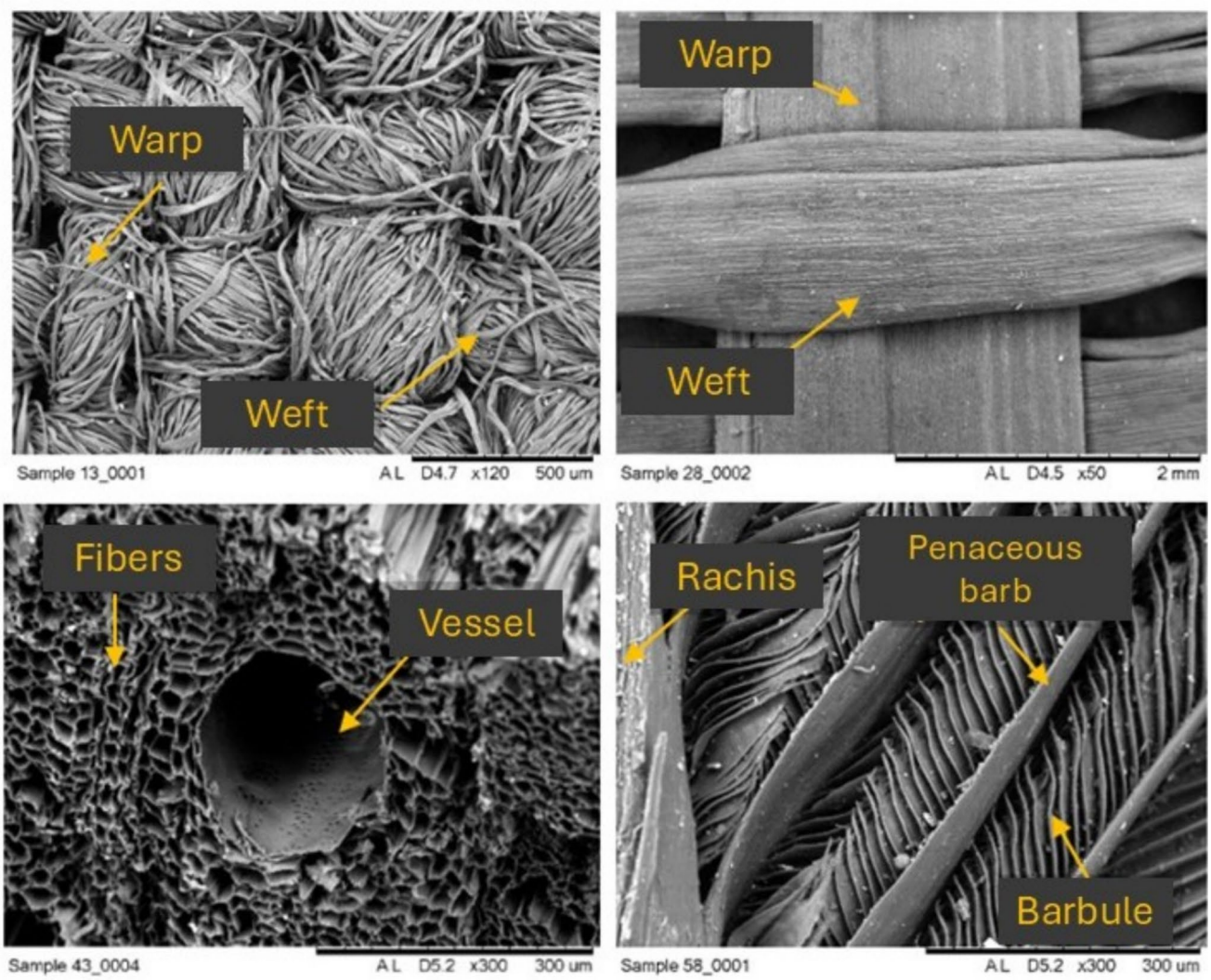

Fig. 11 Monitored areas in cotton, vegetable fiber, wood, and feathers samples mock-ups

Table 6 Comparative efficiency of dry and moist irradiation in pesticide degradation

Pesticide	Analyzed model materials			
	Vegetable Fiber	Wood	Feathers	Cotton
DDT	Wet	Wet	Wet	Dry
HCB	Dry	Dry	Dry	Dry / Wet
γ-HCH	Dry	Dry	Dry	Dry / Wet

The images of the analyzed samples are available in Supplementary Table S8-10.

Table 6 presents a summary of the best irradiation performance for pesticide degradation according to the analyzed samples. The data show that the effectiveness of ionizing radiation in pesticide removal depends not only on the irradiation conditions but also on the physicochemical characteristics of the substrates themselves.

Conclusions

The results demonstrate that gamma irradiation is an effective method for significantly reducing the concentrations of the analyzed organochlorine pesticides and holds considerable potential for the decontamination of cultural heritage materials.

The first experimental phase, conducted with standard solutions, provided fundamental insights into degradation behavior, dose–response relationships, and radiation chemical yields (G-values). The degradation products identified exhibited lower acute toxicity than their parent compounds, supporting the relevance of ionizing radiation as a pesticide

mitigation strategy in heritage conservation. These findings informed the selection of a 30 kGy dose for the second experimental phase using model materials, representing a compromise between effective pesticide degradation and preservation of material integrity.

The degradation efficiency was strongly influenced by both the chemical structure of the pesticides and the characteristics of the substrates. These differences reflect variations in molecular reactivity toward the oxidizing and reducing species generated by ionizing radiation. Highly chlorinated aromatic compounds such as HCB showed a greater propensity for C–Cl bond cleavage through direct radiolysis, whereas non-aromatic saturated molecules such as γ-HCH were more resistant, relying mainly on slower dechlorination reactions.

Substrate properties also affected performance. Porous materials favored higher pesticide removal, while dense or protein-rich matrices limited radical diffusion and interaction. Moist irradiation did not uniformly enhance degradation across all contaminated materials, and its effect varied depending on the availability and mobility of reactive species within each substrate. This condition was particularly beneficial for DDT in materials such as wood, feathers, and vegetable fiber.

Colorimetric, FTIR–ATR, and SEM analyses indicate that irradiation, especially under dry conditions, did not induce severe or readily detectable chemical, chromatic, or structural alterations in the model materials within the sensitivity limits of the applied analytical techniques. However, minor variations were observed in specific cases, particularly under moistened conditions, highlighting the need for cautious interpretation.

Taken together, the combined findings of both experimental phases suggest that gamma irradiation at 30 kGy under dry conditions may offer a controlled and potentially viable approach for the mitigation of organochlorine pesticide contamination in heritage materials, when carefully justified and applied. Given that this dose exceeds those typically used in routine heritage disinfestation practices, its application should be considered on a case-by-case basis, ideally informed by dialogue between conservation professionals and relevant stakeholders, weighing potential secondary effects on materials against the benefits of contaminant reduction, particularly in critical scenarios involving occupational health risks, severely contaminated collections, or repatriation processes where alternative mitigation strategies are limited.

Future research should extend these investigations to a broader range of historical contaminants, additional substrate types, and real contaminated museum objects, as well as include long-term monitoring and a detailed assessment of degradation products formed within solid matrices, in order to further refine irradiation parameters and support the development of evidence-based guidelines for the responsible use of ionizing radiation in cultural heritage pesticide mitigation.

Supplementary Information The online version contains supplementary material available at https://doi.org/10.1007/s10967-025-10700-3.

Acknowledgements The authors gratefully acknowledge the financial support provided by the International Atomic Energy Agency (IAEA) through Research Contract No. 18942 ("Developing Radiation Treatment Methodologies and New Resin Formulations for Consolidation and Preservation of Archived Materials and Cultural Heritage Artefacts") and Project RLA2018012 ("Using Nuclear and Radiation Technology to Characterize, Conserve and Preserve the Cultural Heritage of Latin America and the Caribbean" – ARCAL CLXVII). This research was conducted at the Institute for Energy and Nuclear Research (IPEN), University of São Paulo (USP). We would like to thank the Laboratory of Microscopy and Microanalysis of the Center for Science and Technology of Materials at IPEN/CNEN, Laboratório de Microarqueologia (LabMicro-MAE/USP) for providing access to the FTIR spectrometer and the Museum of Archaeology and Ethnology (MAE-USP) for its support.

Funding International Atomic Energy Agency, 18942, Pablo Antônio Vasquez Salvador, RLA2018012, Pablo Antônio Vasquez Salvador

Declarations

Conflict of interests All authors certify that they have no affiliations with or involvement in any organization or entity with any financial interest or non-financial interest in the subject matter or materials discussed in this manuscript.

References

1. Odegaard N, Sadongei A (2005) Old poisons, new problems: a museum resource for managing contaminated cultural materials. Altamira Press, Walnut Creek
2. Angelova LV, Nawaz S, Kafadaroğlu B, Paz B, Moreta F, Woollaston H, Vermeulen M, Vervoorst J (2023) The use of 'poisonous insecticidal solutions' in bookbinding: coping with historic pesticide treatments in the archive. Herit Sci 11:51. https://doi.org/10.1186/s40494-023-00866-y
3. Basfar AA, Mohamed KA, Al-Saqer OA (2012) De-contamination of pesticide residues in food by ionizing radiation. Radiat Phys Chem 81(4):473–478. https://doi.org/10.1016/j.radphyschem.2011.12.040
4. Brabo PC (2015) Degradação de pesticidas em solos cultivados com café: o uso da radiação gama, CG/EM/EM e a metodologia QuEChERS modificada. Master degree thesis, Instituto Militar de Engenharia, Rio de Janeiro. https://rigeo.sgb.gov.br/jspui/handle/doc/14846
5. Chowdhury MAZ, Jahan I, Karim N, Alam MK, Rahman MA, Moniruzzaman M, Gan SH, Fakhruddin NM (2014) Determination of carbamate and organophosphorus pesticides in vegetable samples and the efficiency of gamma-radiation in their removal. Biomed Res Int 2014:145159. https://doi.org/10.1155/2014/145159/
6. Ciarrocchi IR, Mendes KF, Pimpinato RF, Spoto MHF, Tornisielo VL (2021) The effect of radiation in the degradation of carbendazim and azoxystrobin in strawberry. Radiat Phys Chem 179:109269. https://doi.org/10.1016/j.radphyschem.2020.109269

7. Duarte CL, Mori MN, Kodama Y, Oikawa H, Sampa MHO (2007) Decontamination of pesticide packing using ionizing radiation. Radiat Phys Chem 76(11–12):1885–1889. https://doi.org/10.1016/j.radphyschem.2007.02.108
8. Lépine FL (1991) Effects of ionizing radiation on pesticides in a food irradiation perspective: a bibliographic review. J Agric Food Chem 39:2112–2118. https://doi.org/10.1021/jf00012a002
9. Luchini LC (1995) Degradação do inseticida Paration Etílico em diversas matrizes ambientais por meio da radiação ionizante gama do Cobalto-60. Doctoral thesis, Universidade de São Paulo, Instituto de Química de São Carlos, São Carlos. https://inis.iaea.org/collection/NCLCollectionStore/_Public/31/011/31011549.pdf
10. Mori MN, Oikawa H, Sampa MHO, Duarte CL (2005) Descontaminação de embalagens de clorpirifós utilizando radiação ionizante. In: Proceedings of the International Nuclear Atlantic Conference – INAC 2005, Santos, Brazil, 28 Aug–2 Sep 2005. Associação Brasileira de Energia Nuclear (ABEN). https://www.ipen.br/biblioteca/cd/inac/2005/full/2018.pdf
11. Delgado Vieira AC, Salvador PAV, Oliveira MJA, Wandermuren MN, Cristale J (2026) Evaluation of radiation-induced decontamination of permethrin on model materials for cultural heritage. Radiat Phys Chem 238:113204. https://doi.org/10.1016/j.radphyschem.2025.113204
12. Vasquez P. (2017) Fundamentals of radiation processing technology. In: IAEA. Uses of ionizing radiation for tangible cultural heritage conservation. IAEA, Vienna, pp. 43–50. https://www.iaea.org/publications/10937/uses-of-ionizing-radiation-for-tangible-cultural-heritage-conservation
13. Javaroni RC, Talamoni J, Landgraf MD, Rezende MOO (1991) Estudo da degradação de lindano em solução aquosa através da radiação gama. Quim Nova 14(4):237–239
14. Khedr T, Hammad AA, Elmarsafy AM, Halawa E, Soliman M (2019) Degradation of some organophosphorus pesticides in aqueous solution by gamma irradiation. J Hazard Mater 373:23–28. https://doi.org/10.1016/j.jhazmat.2019.03.011
15. Lippold PC, Cleere JS, Massey LM Jr, Bourke JB, Avens AW (1969) Degradation of insecticides by cobalt-60 gamma radiation. J Econ Entomol 62(6):1509–1510. https://doi.org/10.1093/jee/62.6.1509
16. Delgado Vieira AC, Salvador PAV (2025) The past and present of pest mitigation: results of an international survey of practices. Rev Mus Arqueol Etnol 43:114–128. https://doi.org/10.11606/issn.2448-1750.revmae.2024.227497
17. Dawson J (1988) The effects of insecticides on museum artifacts and materials. In: Zycherman LA, Schrock JR (eds) A guide to museum pest control. Foundation of the American Institute for Conservation of Historic and Artistic Works and Association of Systematics Collections, Washington, DC, pp 135–150
18. Unger A, Schniewind AP, Unger W (2001) Conservation of wood artifacts: a handbook. Springer, Berlin
19. Bangstad TR (2022) Pollution and permanence: museum repair in toxic worlds. Mus Soc Issues 15:13–27. https://doi.org/10.1080/15596893.2022.2083356
20. Urkude R (2019) Pesticide residues in beverages. In: Grumezescu AM, Holban AM (eds) Quality control in the beverage industry. Elsevier, Oxford, pp 529–560. https://doi.org/10.1016/C2017-0-02391-1
21. Plenderleith HJ, Werner AEA (1971) The conservation of antiquities and works of art: treatment, repair and restoration. Oxford University Press, London
22. ICOM (1965) Problems of conservation in museums. Eyrolles, Paris, Travaux et Publications VIII, pp 89–92
23. Hueck HJ (1972) Textile conservation. Textile pests and their control. Butterworth & Co, London, pp 87–89
24. Kühn H (1986) Conservation and restoration of works of art and antiquities. Butterworth & Co, London, pp 229–230
25. Pinniger DB (2001) Pest management in museums, archives and historic houses. Archetype Publications, London
26. Ioannou N, Da Ros S (2025) An assessment of integrated pest management awareness in heritage institutions. Stud Conserv 70(4):306–316. https://doi.org/10.1080/00393630.2024.2375152
27. Mackay D, Shiu WY, Ma KC, Lee SC (2006) Handbook of physical-chemical properties and environmental fate for organic chemicals, 2nd edn. CRC Press, Boca Raton
28. Salmo R, Palmer PT, Tribe K (2017) Fast, nondestructive, and cost-effective methods to detect pesticide residues: a case study of several repatriated Karuk Tribe artifacts. Collect Forum 31(1–2):23–33. https://doi.org/10.14351/0831-4985-31.1.23
29. Uden J, Charlton A, Domoney K (2014) The analysis of pesticide residues on the Cook-Voyage Collections in the Pitt Rivers Museum, University of Oxford. In: ICOM Committee for Conservation 17th Triennial Meeting, Melbourne, Australia, 19–23 Sep 2014. https://www.icom-cc-publications-online.org/1380/The-Analysis-of-Pesticide-Residues-on-the-Cook-Voyage-Collections-in-the-Pitt-Rivers-Museum-University-of-Oxford
30. Goldberg LA (1996) History of pest control measures in the anthropology collections, National Museum of Natural History, Smithsonian Institution. J Am Inst Conserv 5(1):23–43. https://doi.org/10.1179/019713696806124601
31. Hawks C, Makos K (2000) Inherent hazards in museum collections. CRM 5:31–37
32. Ornstein L (2010) Poisonous heritage: pesticides in museum collections. Master of Arts thesis, Seton Hall University, New Jersey. https://scholarship.shu.edu/theses/253
33. Tello H (2021) Les insecticides, témoins silencieux dans les collections du Musée d'ethnologie de Berlin: Les collections muséales du Musée d'ethnologie de Berlin entre preservation et délabrement. Trouble dans les collections, Musée Théodore Monod de l'IFAN (Dakar).https://halshs.archives-ouvertes.fr/halshs-03407895
34. Sadongei A (2001) American Indian concepts of object use. Collect Forum 17(1–2):113–116
35. Getoff N, Solar S (1988) Radiation induced decomposition of chlorinated phenols in water. Radiat Phys Chem 31(1–3):121–130. https://doi.org/10.1016/1359-0197(88)90115-4
36. Spinks JWT, Woods RJ (1990) An introduction to radiation chemistry, 3rd edn. John Wiley, New York
37. Burrows HD, Canle LM, Santaballa JA, Steenken S (2002) Reaction pathways and mechanisms of photodegradation of pesticides. J Photochem Photobiol B 67(2):71–108. https://doi.org/10.1016/S1011-1344(02)00277-4
38. Abdel Aal S, Dessouki A, Sokker H (2001) Degradation of some pesticides in aqueous solutions by electron beam and gamma-radiation. J Radioanal Nucl Chem 250:329–334. https://doi.org/10.1023/A:1017912132599
39. Ghaffar A, Masaaki T, Aziz R, Sarfraz S (2023) Catalytic degradation of lindane using gamma radiations: degradation products. Radiat Phys Chem 205:110741. https://doi.org/10.1016/j.radphyschem.2022.110741
40. Mohamed KA, Basfar AA, Al-Kahtani HA, Al-Hamad KS (2009) Radiolytic degradation of malathion and lindane in aqueous solutions. Radiat Phys Chem 78:994–1000. https://doi.org/10.1016/j.radphyschem.2009.06.003
41. Unger A (2012) Decontamination and "deconsolidation" of historical wood preservatives and wood consolidants in cultural heritage. J Cult Herit 13S:196-S202. https://doi.org/10.1016/j.culher.2012.01.015
42. Shugar AN, Sirois PJ (2012) Handheld XRF use in the identification of heavy metal pesticides in ethnographic collections. In: Shugar AN, Mass JL (eds) Handheld XRF for art and archaeology. Leuven University Press, UK, pp 313–348. https://doi.org/10.2307/j.ctt9qdzfs.13

43. PPDB Pesticide Properties Database (2025) Creating tools for pesticide risk assessment and management in Europe Developed by the Agriculture & Environment Research Unit (AERU), University of Hertfordshire. https://sitem.herts.ac.uk/aeru/ppdb/en/index.htm
44. Quye A, Strlič M (2019) Ethical sampling guidance. Icon Heritage Science Group, ICON, pp. 1–14. https://www.icon.org.uk/static/3e959f66-580b-406c-a5fce17367aa4c13/iconhsgethicalsamplingguidance-jan2019.pdf
45. Instituto Nacional de Metrologia, Qualidade e Tecnologia (INMETRO) (2020) Orientação sobre validação de métodos analíticos–DOQ-CGCRE-008. Coordenação Geral de Acreditação, Brasília. https://www.gov.br/cdtn/pt-br/assuntos/documentos-cgcre-abnt-nbr-iso-iec-17025/doq-cgcre-008/view
46. Peters FT, Olaf HD, Musshoff F (2007) Validation of new methods. Forensic Sci Int 165:216–224. https://doi.org/10.1016/j.forsciint.2006.05.021
47. Ribani M (2004) Validação em métodos cromatográficos e eletroforéticos. Quim Nova 27(5):771–780. https://doi.org/10.1590/S0100-40422004000500017
48. EC European Commission (2021). Guidance document on analytical quality control and method validation procedures for pesticide residues and analysis in food and feed (SANTE/11312/2021). https://www.eurl-pesticides.eu/userfiles/file/EurlALL/S ANTE_11312_2021.pdf
49. Getoff N (1996) Radiation induced degradation of water pollutants—state of the art. Radiat Phys Chem 47:581–593. https://doi.org/10.1016/0969-806X(95)00059-7
50. Kurucz CN, Waite TD, Cooper WJ, Nickelsen MG (1991) High energy electron beam irradiation of water, wastewater and sludge. In: Lewins J, Becker M (eds) Advances in nuclear science and technology. Plenum Press, New York, pp 1–43. https://doi.org/10.1007/978-1-4615-3392-4_1
51. Hardeberg JY (2001) Acquisition and reproduction of color images, colorimetric and multispectral approaches. Dissertation.com, USA. https://bookpump.com/bwp/pdf-b/1121350b.pdf
52. Mincher BJ, Meikrantz DH, Murphy RJ, Gresham GL, Connolly MJ (1991) Gamma-ray induced degradation of PCBs and pesticides using spent reactor fuel. Int J Radiat Appl Instrum A Appl Radiat Isot 42(11):1061–1066. https://doi.org/10.1016/0883-2889(91)90011-O
53. Shammi M, Uddin MK, Malek MA, Hasanuzzaman M (2009) Persistent organic pollutants (POPs) management in Bangladesh: gamma radiation induced degradation of obsolete pesticide DDT and its metabolites DDD and DDE. Jahangirnagar Univ J Sci 32:43–51
54. Yongke H, Hongtao C, Xiangrong S, Jilan W (1993) Radiation-induced dechlorination of hexachlorobenzene. Radiat Phys Chem 42(4–6):715–717. https://doi.org/10.1016/0969-806X(93)90358-2
55. Zhang J, Zheng Z, Luan J, Yang G, Song W, Zhong Y, Xie Z (2007) Degradation of hexachlorobenzene by electron beam irradiation. J Hazard Mater 142:431–436. https://doi.org/10.1016/j.jhazmat.2006.08.035
56. Khan S (2014) Removal of lindane from water using advanced oxidation techniques. Doctoral thesis, University of Peshawar, Peshawar, Pakistan. https://prr.hec.gov.pk/jspui/bitstream/123456789/8045/1/SANAULLAH_KHAN_2015_PHYSICAL_CHEMISTRY_University_of_Peshawar_29_04_2016.pdf
57. Srivastava S, Goyal P, Srivastava MM (2010) Pesticides: past, present, and future. In: Nollet LML, Rathore HS (eds) Handbook of pesticides: methods of pesticide residues analysis. CRC Press, Boca Raton, pp 47–65
58. Zacharia JT (2011) Identity, physical and chemical properties of pesticides. In: Stoytcheva M (ed) Pesticides in the modern world: trends in pesticides analysis. IntechOpen, London, pp 1–18. https://doi.org/10.5772/17513
59. Trojanowicz M (2020) Removal of persistent organic pollutants (POPs) from waters and wastewaters by the use of ionizing radiation. Sci Total Environ 718:134425. https://doi.org/10.1016/j.scitotenv.2019.134425
60. Meshitsuka G, Burton M (1958) Radiolysis of liquid methanol by Co-60 gamma-radiation. Radiat Res 8(4):285–297. https://doi.org/10.2307/3570468
61. Barker R (1962) Gamma-radiolysis of liquid acetone. Trans Faraday Soc 59:375–385. https://doi.org/10.1039/TF9635900375
62. Hodgson E, Roe RM, Chambers JE (2005) Dictionary of toxicology, 3rd edn. Elsevier Academic Press, Oxford
63. UNEP – United Nations Environment Programme (2017) Stockholm convention on persistent organic pollutants (POPs): Texts and Annexes. 4th edn Geneva: Secretariat of the Stockholm Convention. https://www.pops.int/
64. Dessouki AM, Aly HF, Sokker HH (1999) The use of gamma radiation for removal of pesticides from waste water. Czech J Phys 49:521–533. https://doi.org/10.1007/s10582-999-0071-y
65. LaVerne JA, Driscoll MS, Al-Sheikhly M (2020) Radiation stability of lignocellulosic material components. Radiat Phys Chem 171:108716. https://doi.org/10.1016/j.radphyschem.2020.108716
66. Łojewski T, Miśkowiec P, Missori M, Lubańska A, Proniewicz LM, Łojewska J (2010) FTIR and UV/vis as methods for evaluation of oxidative degradation of model paper: DFT approach for carbonyl vibrations. Carbohydr Polym 82:370–375. https://doi.org/10.1016/j.carbpol.2010.04.087
67. Emam AS, Shouman MG, Mohamed MF (2019) Using FTIR to study the chemical degradation of archaeological wood in EL-Moez Street. Int J Multidiscip Stud Archit Cult Herit 3:81–94. https://doi.org/10.21608/ijmsac.2019.182200
68. Margariti C (2019) The application of FTIR microspectroscopy in a non-invasive and non-destructive way to the study and conservation of mineralized excavated textiles. Herit Sci 7:63. https://doi.org/10.1186/s40494-019-0304-8
69. Cemmi A, Sarcina ID, D'Orsi B (2023) Gamma radiation-induced effects on paper irradiated at absorbed doses common for cultural heritage preservation. Radiat Phys Chem 202:110452. https://doi.org/10.1016/j.radphyschem.2022.110452
70. Wang Y, Chen Q, Lei Y, Kaya MGA, Goh KL, Tang K (2025) Identification, deterioration, and protection of organic cultural heritages from a modern perspective. NPJ Herit Sci 13:71. https://doi.org/10.1038/s40494-025-01601-5
71. Sionkowska A, Skopińska-Wiśniewska J, Kozłowska J, Płanecka A, Kurzawa M (2011) Photochemical behaviour of hydrolysed keratin. Int J Cosmet Sci 33:312–317. https://doi.org/10.1111/j.1468-2494.2011.00662.x
72. Vyskočilová G, Ebersbach M, Kopecká R, Prokeš L, Příhoda J (2019) Model study of the leather degradation by oxidation and hydrolysis. Herit Sci 7:26. https://doi.org/10.1186/s40494-019-0269-7
73. Vadrucci M, Cicero C, Mazzuca C, Severini L, Uccelletti D, Schifano E, Mercuri F, Zammit U, Orazi N, D'Amico F, Parisse P (2023) Evaluation of the irradiation treatment effects on ancient parchment samples. Heritage 6:1308–1324. https://doi.org/10.3390/heritage6020072
74. Łojewski T, Mis´Kowiec P, Missori M, Lubańska A, Proniewicz LM, Łojewska J (2010) FTIR and UV/vis as methods for evaluation of oxidative degradation of model paper: DFT approach for carbonyl vibrations. Carbohydr Polym 82:370–375. https://doi.org/10.1016/j.carbpol.2010.04.087

75. Sistach MC, Ferrer N, Romero MT (1998) Fourier transform infrared spectroscopy applied to the analysis of ancient manuscripts. Restaurator 19:173–186. https://doi.org/10.1515/rest.1998.19.4.173

Authors and Affiliations

Ana Carolina Delgado Vieira[1,2] · Pablo A. S. Vasquez[2] · Maria José Alves de Oliveira[2] · Marcio Nardelli Wandermuren[3] · Joyce Cristale[4]

✉ Ana Carolina Delgado Vieira
ana.carolina.vieira@usp.br

[1] Museu de Arqueologia E Etnologia [Museum of Archeology and Ethnology], University of São Paulo (MAE / USP), Av. Professor Almeida Prado, 1466, São Paulo, SP 05508-070, Brazil

[2] Instituto de Pesquisas Energéticas E Nucleares [Nuclear and Energy Research Institute] (IPEN / CNEN), Av. Professor Lineu Prestes, 2242, São Paulo, SP 05508-000, Brazil

[3] Instituto de Química [Institute of Chemistry], University of São Paulo (IQ / USP), Av. Professor Lineu Prestes, 748, São Paulo 05508-000, Brazil

[4] Centro Pluridisciplinar de Pesquisas Químicas, Biológicas E Agrícolas, Universidade Estadual de Campinas – UNICAMP, Av. Alexandre Cazellato, 999, Paulínia 13148-218, Brazil